AMERICAN SOCIETY FOR MICROBIOLOGY | Journal of Virology®

VIRUS-CELL INTERACTIONS

Mutations in Hypervariable Domain of Venezuelan Equine Encephalitis Virus nsP3 Protein Differentially Affect Viral Replication

Chetan D. Meshram,[a] Aaron T. Phillips,[a] Tetyana Lukash,[a] Nikita Shiliaev,[a] Elena I. Frolova,[a] Ilya Frolov[a]

[a]Department of Microbiology, University of Alabama at Birmingham, Birmingham, Alabama, USA

ABSTRACT Venezuelan equine encephalitis virus (VEEV) is one of the important human and animal pathogens. It forms replication enzyme complexes (RCs) containing viral nonstructural proteins (nsPs) that mediate the synthesis of virus-specific RNAs. The assembly and associated functions of RC also depend on the presence of a specific set of host proteins. Our study demonstrates that the hypervariable domain (HVD) of VEEV nsP3 interacts with the members of the FXR family of cellular proteins and also binds the Src homology 3 (SH3) domain-containing proteins CD2AP and SH3KBP1. Interactions with FXR family members are mediated by the C-terminal repeating peptide of HVD. A single short, minimal motif identified in this study is sufficient for driving efficient VEEV replication in the absence of HVD interactions with other host proteins. The SH3 domain-containing proteins bind to another fragment of VEEV HVD. They can promote viral replication in the absence of FXR-HVD interactions albeit less efficiently. VEEV replication can be also switched from an FXR-dependent to a chikungunya virus-specific, G3BP-dependent mode. The described modifications of VEEV HVD have a strong impact on viral replication *in vitro* and pathogenesis. Their effects on viral pathogenesis depend on mouse age and the genetic background of the virus.

IMPORTANCE The replication of alphaviruses is determined by specific sets of cellular proteins, which mediate the assembly of viral replication complexes. Some of these critical host factors interact with the hypervariable domain (HVD) of alphavirus nsP3. In this study, we have explored binding sites of host proteins, which are specific partners of nsP3 HVD of Venezuelan equine encephalitis virus. We also define the roles of these interactions in viral replication both *in vitro* and *in vivo*. A mechanistic understanding of the binding of CD2AP, SH3KBP1, and FXR protein family members to VEEV HVD uncovers important aspects of alphavirus evolution and determines new targets for the development of alphavirus-specific drugs and directions for viral attenuation and vaccine development.

KEYWORDS CD2AP, FMRP, FXR1, FXR2, SH3KBP1, Venezuelan equine encephalitis virus, viral pathogenesis, alphaviruses, intrinsically disordered proteins, nsP3

The *Alphavirus* genus in the *Togaviridae* family contains a wide variety of human and animal pathogens, which are present on all continents (1). Based on geographical distribution, alphaviruses are divided into New World (NW) and Old World (OW) species. The NW alphaviruses most relevant to human health are exemplified by Venezuelan (VEEV), eastern (EEEV), and western (WEEV) equine encephalitis viruses (2, 3). They are highly pathogenic and in humans, induce debilitating diseases characterized by severe meningoencephalitis that may result in lethal outcomes or neurological sequelae (4). Naturally circulating encephalitogenic NW alphaviruses are lethal for equids and in small-animal models. They can replicate to high titers in many commonly used cell lines

Citation Meshram CD, Phillips AT, Lukash T, Shiliaev N, Frolova EI, Frolov I. 2020. Mutations in hypervariable domain of Venezuelan equine encephalitis virus nsP3 protein differentially affect viral replication. J Virol 94:e01841-19. https://doi.org/10.1128/JVI.01841-19.

Editor Susana López, Instituto de Biotecnologia/UNAM

Address correspondence to Ilya Frolov, ivfrolov@uab.edu.

Received 28 October 2019
Accepted 30 October 2019
Accepted manuscript posted online 6 November 2019
Published 17 January 2020

of vertebrate and mosquito origins, are highly stable in lyophilized form, and can be very efficiently transmitted by aerosol (5). There is a possibility for the application of VEEV and other NW alphaviruses in biological warfare. Therefore, they are classified as category B select agents by the CDC. Despite public health and national security threats, to date, no licensed vaccines and therapeutic means have been developed for VEEV and other NW alphaviruses.

The VEEV genome is a single-stranded ~11.5-kb RNA of positive polarity (6, 7). It mimics the structure of cellular mRNAs, in that it contains a cap at the 5′ terminus and a poly(A) tail at the 3′ terminus (1, 8). The genomic RNA (G RNA) encodes only a few proteins. Four viral nonstructural proteins (nsP1 to -4) are translated directly from G RNA and function in RNA replication and transcription of the subgenomic RNA (SG RNA) (1, 9). The latter SG RNA is translated into viral structural proteins, which ultimately form G RNA-containing, infectious virions.

The distribution of alphaviruses in different geographical areas led to their adaptation to specific mosquito species that serve as transmitting vectors and vertebrates that are used by alphaviruses as amplifying hosts during natural viral circulation. This adaptation is strongly determined by the evolution of viral structural proteins. They mediate viral interactions with cellular receptors and, ultimately, the delivery of G RNA into the cytoplasm. To date, alphavirus evolution has resulted in the development of at least four serocomplexes with ~40% identity in the amino acid sequences of the envelope glycoproteins (1). In contrast to viral structural proteins, the nonstructural proteins are more conserved. Their evolution is constrained by enzymatic functions of the nsPs in the synthesis and posttranscriptional modifications of virus-specific G and SG RNAs. The catalytic activities of nsP1, nsP2, and nsP4 have been relatively well characterized (10–17). However, the roles of nsP3, and VEEV nsP3 in particular, in viral replication remain poorly understood. The nsP3 protein contains two conserved, structured N-terminal domains, the macrodomain and the alphavirus unique domain (AUD) (18, 19). As do other nsPs, these domains demonstrate a high level of conservation between viral species. The macrodomain exhibits mono-ADP-ribosylhydrolase activity (18, 20–22). The mutations introduced into Sindbis virus (SINV) and chikungunya virus (CHIKV) macrodomains affect the pathogenesis of the viruses (22) and the ability to inhibit cellular translation in *in vitro* experiments (23–25). Some of the mutations in AUD were shown to have deleterious effects on the synthesis of SG RNA, suggesting its function in the regulation of the activity of the SG promoter (26). AUD can also acquire adaptive mutations that can partially compensate for the negative effects of amino acid substitutions in other domains and increase the replication of viral G RNA (27) (data not shown). The last, C-terminal domain in alphavirus nsP3 is highly variable in both length and amino acid sequence. Therefore, it was termed a hypervariable domain (HVD). In all studied alphaviruses, it is also phosphorylated (27–30), but the role of this posttranslational modification in viral replication remains to be understood. The most recent studies demonstrated that (i) HVD is a prerequisite for the replication of G RNA of VEEV and other alphaviruses (27, 31, 32), (ii) alphavirus HVDs contain multiple linear motifs that interact with sets of host factors in virus- and cell-specific modes (33–36), (iii) HVDs function as hubs for recruiting cellular proteins during replication complex (RC) assembly at the plasma membrane (37), and (iv) the high variability of alphavirus HVDs suggests that their evolution may play a critical role in viral adaptation to new species of hosts and/or mosquito vectors. HVDs of the OW alphaviruses, such as CHIKV, SINV, and Semliki Forest virus (SFV), were found to interact with both members of the G3BP family of cellular proteins, G3BP1 and G3BP2, via a short, conserved, C-terminal, repeating peptide (34, 38, 39). HVDs of the NW alphaviruses, which include VEEV and EEEV, interact with all three FXR family members, FXR1, FXR2, and FMRP (31). The EEEV HVD also binds both G3BP proteins (33). These interactions are critical determinants of RC formation and the synthesis of viral RNAs. Other host factors that demonstrate binding to VEEV HVD include CD2AP and SH3KBP1 (33, 34). The interaction of the latter Src homology 3 (SH3) domain-containing proteins with CHIKV HVD has been previously characterized by nuclear magnetic resonance

(NMR), and its biological function in viral RC formation has been established (40). However, CHIKV/SINV and VEEV HVDs fundamentally differ in amino acid sequences and spectra of binding host factors (33, 34, 41); the mechanistic data obtained for CHIKV and SINV HVD functions in viral RNA replication are not directly applicable to the VEEV counterpart. Therefore, in this study, we have analyzed the host protein-binding motifs in VEEV nsP3 HVD and the roles of HVD-interacting host partners in viral replication and pathogenesis.

RESULTS

Mapping of the host factor-binding sites in VEEV HVD. In our previous studies (31, 33), we applied coimmunoprecipitation (co-IP) followed by mass spectrometry analysis to identify host factors that interact with VEEV nsP3 HVD. In murine NIH 3T3 cells, the VEEV-specific HVD was found to efficiently bind two SH3 domain-containing proteins, CD2AP and SH3KBP1. All three members of the FXR protein family (FXR1, FXR2, and FMR1) were also identified as major and specific HVD-interacting host factors. A few other host proteins were detected in co-IP samples, but their levels were relatively low. To continue the investigation of HVD interactions and map the binding sites of the identified host proteins, we applied SINV-based replicons (SINrep) to express HVD of VEEV fused with green fluorescent protein (GFP) containing Flag at the N terminus (Flag-GFP-HVDveev). The basic construct encoded the entire 220-amino-acid (aa)-long VEEV HVD (aa 330 to 550 of nsP3). In others, HVD was divided into 3 fragments (fragments A, B, and C). In these fragments, we changed the order of amino acids, closely located in the wild-type (wt) sequence, to modify the binding motifs without alteration of the predicted disordered structure and hydrophobicity profile of HVD. For simplicity of presentation, the modified A, B, and C fragments were labeled 1, 2, and 3, respectively. The designed constructs are schematically presented in Fig. 1A. An additional HVD (ABCΔRep) had a wt amino acid sequence with only the C-terminal amino acid repeat deleted, and it retained the 13-aa-long peptide of fragment C, which is located upstream of the repeat in wt HVD.

The *in vitro*-synthesized SINV-based replicons and helper SINV RNAs were coelectroporated into BHK-21 cells, and the collected replicon-containing viral particles were used to infect NIH 3T3 and HEK 293 cells at the same multiplicity of infection (MOI) of 20 infectious units (inf.u)/cell. Cells were harvested at 3 h postinfection (p.i.), after the time when GFP expression became visible under a fluorescence microscope. VEEV nsP3 HVD-containing protein complexes were isolated using magnetic beads loaded with a Flag-specific monoclonal antibody (MAb) (see Materials and Methods for details). Their contents were analyzed by Western blotting using CD2AP-, SH3KBP1-, and FXR1-specific antibodies (Abs) (Fig. 1B). The results of the analysis can be summarized as follows: (i) the binding patterns of host proteins that bind to VEEV HVD in human HEK 293 cells and mouse NIH 3T3 cells are alike; (ii) CD2AP and SH3KBP1 interact with wt fragment B of the HVD (aa 392 to 464 of nsP3), but additional weak binding of both proteins to fragment C is also detectable; and (iii) both human and mouse FXR1 proteins interact with fragment C. This binding is mediated by the C-terminal repeat because its deletion in the fusion protein expressed by SINrep/Flag-GFP-HVDΔRep makes it incapable of interaction. A defined map of HVD-specific binding sites is presented in Fig. 1C.

Lack of binding sites for host factors in VEEV HVD affects viral replication. In our previous studies (31, 41), the engineered VEEV variants, which had the entire HVD either deleted or replaced with heterologous sequences, were not viable. Thus, VEEV HVD plays a critical role(s) in driving viral replication, but the mechanism of its function remained unclear.

To continue the investigation of VEEV nsP3 HVD structure and function, we used the above-described data on mapping of the binding sites (Fig. 1C) of host proteins and designed a set of VEEV TC-83 mutants with strongly modified HVDs (Fig. 2A and B). The recombinant genomes contained the gene for GFP under the control of the subgenomic promoter to monitor the numbers of infected cultured cells and viral spread.

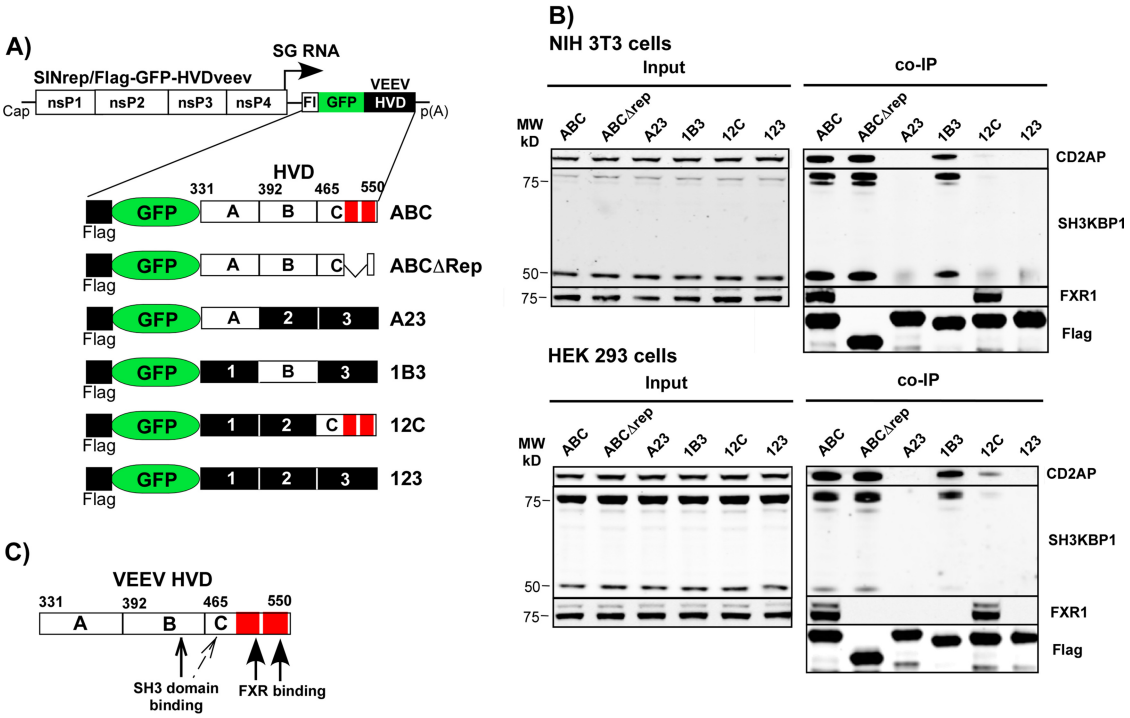

FIG 1 VEEV nsP3 HVD interacts with murine and human FXR1 and SH3 domain-containing proteins via different fragments. (A) Schematic presentation of the designed SINV replicons and the encoded different fusions of Flag-GFP-HVD. Fragments with wt amino acid sequences are indicated by A, B, and C. The corresponding mutated fragments are labeled 1, 2, and 3, respectively. The elements of the C-terminal repeat in VEEV HVD are indicated by red boxes. Numbers indicate positions of amino acids in VEEV nsP3. Fl indicates position of Flag. (B) NIH 3T3 and HEK 293 cells were infected at an MOI of 20 inf.u/cell with viral particles containing SINV replicons encoding the indicated fusion proteins. Protein complexes were isolated using magnetic beads loaded with Flag-specific MAbs as described in Materials and Methods. Complexes were analyzed by Western blotting using the indicated primary and corresponding secondary Abs. Membranes were scanned on a Li-Cor imager. MW, molecular weight. (C) Schematic presentation of the positions of binding sites of the indicated host proteins in VEEV HVD.

The parental VEEV/GFP encoded wt nsP3 HVD. The VEEV/artHVD/GFP variant had the entire HVD mutated (artificial HVD) and was incapable of interaction with the SH3 domain-containing host proteins and FXR family members. The encoded HVD was similar to that in the FlagGFP123 cassette presented in Fig. 1A. However, in addition to changing the positions of closely located amino acids, all serines and threonines in artHVD were replaced by other noncharged, hydrophilic amino acids (glycines and alanines) to eliminate potential sites of phosphorylation. Another mutant, VEEV/Rep/GFP, encoded only one element of the C-terminal VEEV HVD-specific repeat, which was left in the context of the above-described artHVD (Fig. 2A and B). Prolines in the short amino acid sequence corresponding to fragment C located upstream of the retained element of the repeat were replaced by alanines (Fig. 2A). The latter mutations were introduced to affect the detected weak interaction with SH3 domain-containing proteins described above. A third variant with a mutated HVD, VEEV/ΔRep/GFP, encoded the wt HVD sequence, except that both elements of the C-terminal repeat, which mediate the interaction with FXR family members, were deleted (Fig. 2A and B). Thus, the replication of the designed constructs was expected to be either (i) dependent on all HVD-binding motifs (VEEV/GFP) or (ii) determined by only a single element of the repeat that mediates interactions with FXR family members in the absence of interactions with CD2AP, SH3KBP1, and other possible SH3 domain-containing proteins (VEEV/Rep/GFP), or (iii) the replication of VEEV/ΔRep/GFP was determined by HVD interactions with CD2AP and SH3KBP1 in the absence of interactions with the proteins of the FXR family.

The above-described viral genomes were synthesized *in vitro* from plasmid DNAs, and BHK-21 cells were electroporated with equal amounts of RNAs. In an

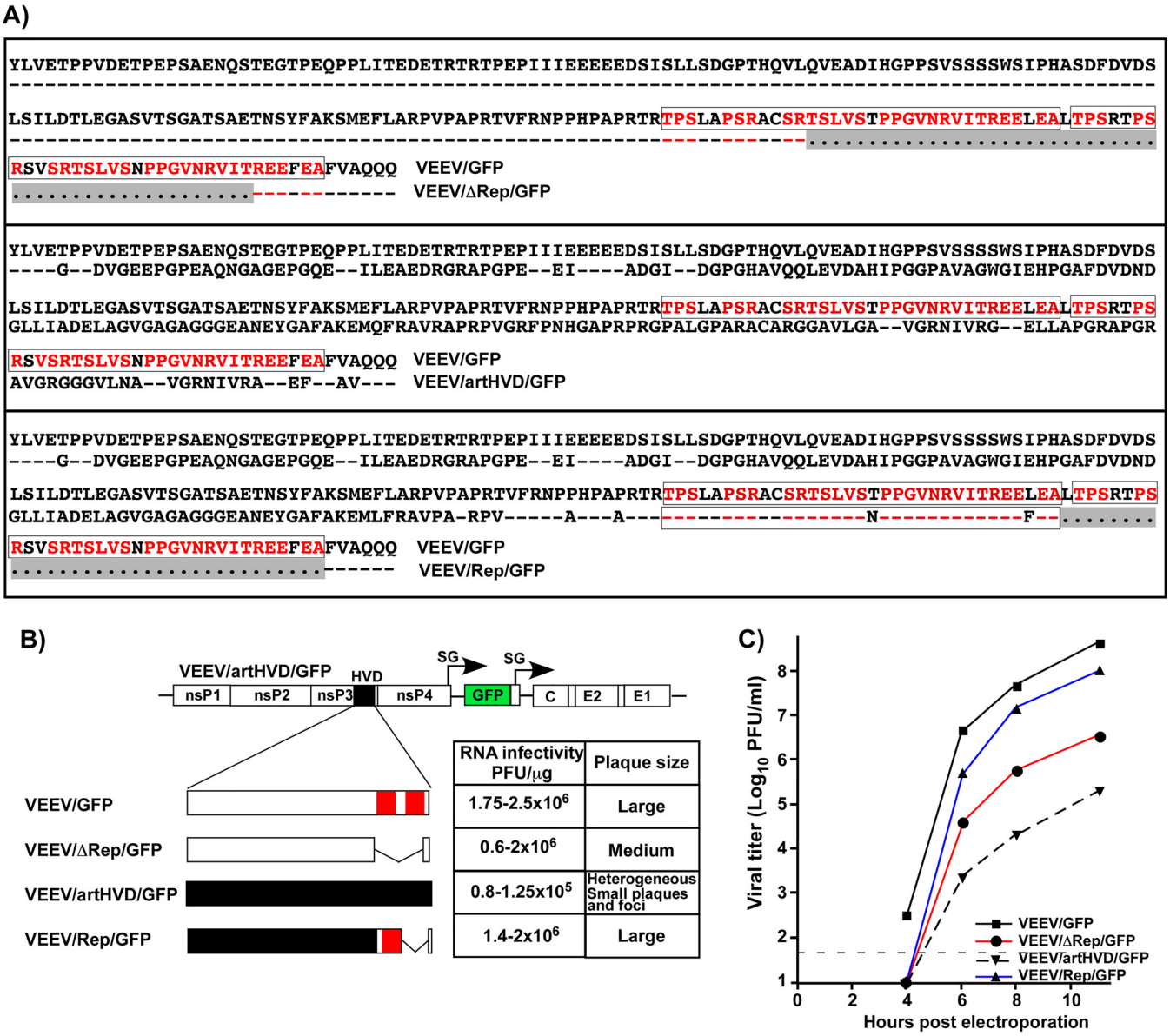

FIG 2 Lack of host protein-binding motifs in VEEV HVD differentially affects viral replication. (A) Alignments of wt and mutated VEEV HVDs. Sequences of two elements of the repeat are indicated in red. Deleted amino acids are indicated by dots on a gray background. (B) Schematic presentation of designed HVDs, infectivities of the *in vitro*-synthesized G RNAs in ICAs, and comparative plaque sizes. wt amino acid sequences are indicated by open boxes, and mutated sequences are indicated by black boxes. Red boxes show positions of the elements of the C-terminal repeat. (C) BHK-21 cells were electroporated with 3 μg of the *in vitro*-synthesized RNAs. Media were collected at the indicated time points, and viral titers were determined by a plaque assay on BHK-21 cells. This experiment was performed twice, with reproducible differences. The results of one of the experiments are presented.

infectious center assay (ICA), VEEV/artHVD/GFP RNA reproducibly demonstrated 10-fold-lower infectivity (Fig. 2B) and produced a mixture of both small foci of GFP-positive cells and very small plaques of noticeably heterogeneous sizes (Fig. 2B). The lower RNA infectivity was an indication of the inefficient initiation of RNA replication. As in the above-described studies, the heterogeneity of plaques/foci suggested rapid viral evolution and the generation of numerous variants that can replicate in BHK-21 cells. However, at any time postelectroporation, titers of the released VEEV/artHVD/GFP progeny remained 3 to 4 orders of magnitude below those of parental VEEV/GFP (Fig. 2C). In repeat experiments, RNA infectivities of other variants, VEEV/Rep/GFP and VEEV/ΔRep/GFP, were essentially the same as those of parental VEEV/GFP (Fig. 2B), and plaques were homogeneous. Compared to VEEV/GFP, the variant that lacked the C-terminal amino acid repeat, VEEV/ΔRep/

GFP, demonstrated low rates of replication (Fig. 2C), which correlated with its small plaques formed on BHK-21 cells (Fig. 2B). VEEV/Rep/GFP, in contrast, replicated with an efficiency comparable to that of parental VEEV/GFP (Fig. 2B and C).

These results demonstrated that (i) the lack of all protein-binding motifs in the HVD had a deleterious effect on the replication of the VEEV/artHVD/GFP mutant and induced rapid viral evolution to a more efficiently replicating phenotype, (ii) the presence of a single VEEV HVD-specific element of the FXR protein family-binding repeat in the context of the artificially designed HVD had a strong positive impact on viral replication, and (iii) the deletion of the C-terminal repeating peptide in wt VEEV nsP3 HVD had a profound negative effect on viral replication. However, importantly, the deletion did not make virus nonviable. This was an indication that interactions with host proteins, most likely with CD2AP and SH3KBP1, were capable of facilitating VEEV replication in the absence of FXR binding albeit not to the wt level.

Mapping of the functional peptide in the repeating element of VEEV HVD. The above-described and our previous (27) data strongly suggested that the C-terminal FXR-binding repeat in VEEV HVD plays a critical role in viral replication. Each element of this repeat is 33 aa long. These peptides are significantly longer than the previously identified ~6-aa-long repeating peptides that mediate interactions of the OW alphavirus HVDs with G3BP proteins (31, 39). Moreover, the FXR-interacting peptide found in the HVD of another NW alphavirus, EEEV (33), demonstrates a readily detectable level of identity with its VEEV-specific counterpart but also appears to be shorter (Fig. 3A). Therefore, in the next experiments, we further mapped the amino acid sequence in the VEEV HVD repeat that is sufficient for supporting viral replication.

First, we additionally modified the VEEV/Rep/GFP mutant. The new variant, termed VEEV/minRep/GFP, also encoded artHVD with a single copy of the FXR-binding motif. However, the 10-aa-long fragment of the original single repeat was deleted to make it similar to the FXR-binding counterpart of EEEV HVD (Fig. 3B). The replication of the newly designed VEEV/minRep/GFP recombinant virus was compared to that of the above-described parental VEEV/Rep/GFP, which encoded in its HVD a single complete element of the repeat. The *in vitro*-synthesized RNAs of both VEEV/minRep/GFP and VEEV/Rep/GFP were electroporated into BHK-21 cells, and the release of the viruses was assessed at different times posttransfection (Fig. 3C). No differences in viral replication rates and final infectious titers were detected. Hence, we concluded that the designed shorter motif was supporting VEEV replication as efficiently as the natural full-length FXR-interacting peptide.

Next, we introduced a series of small deletions into a minRep peptide-coding sequence and evaluated their effects on viral replication. The designed deletions are presented in Fig. 4A. Equal amounts of the *in vitro*-synthesized mutant RNAs were electroporated into BHK-21 cells to assess their infectivities and viral titers at 24 h posttransfection. Each small 3-aa-long deletion in the proposed minimal peptide but not in the upstream-located amino acid sequence (Δ0) had negative effects on RNA infectivity (Fig. 4B) and virus release (Fig. 4C). Plaques formed by the deletion mutants also became very small (data not shown). These results strongly suggested that all of the amino acids in the peptide exhibiting a high level of identity with the EEEV-specific FXR-binding motif (Fig. 3A and Fig. 4A) are critical for viral replication. Thus, the size of the proposed FXR-interacting minimal peptide cannot be further reduced without compromising viral replication.

The designed Δ1 to Δ6 viral mutants were similar to VEEV/artHVD/GFP (Fig. 2) in terms of reaching low infectious titers at 24 h p.i. (PFU per milliliter) and the development of pinpoint plaques. As did VEEV/artHVD/GFP, most of the mutants demonstrated noticeable evolution to higher replication rates and a larger-plaque-forming phenotype. After an additional passage of electroporation-derived viral samples on BHK-21 cells, we purified viruses from large plaques formed by VEEV variants with Δ1, Δ2, and Δ3 deletions in the nsP3-specific HVD and sequenced viral nonstructural genes. The putative adaptive mutations were detected in either the nsP2 helicase and protease

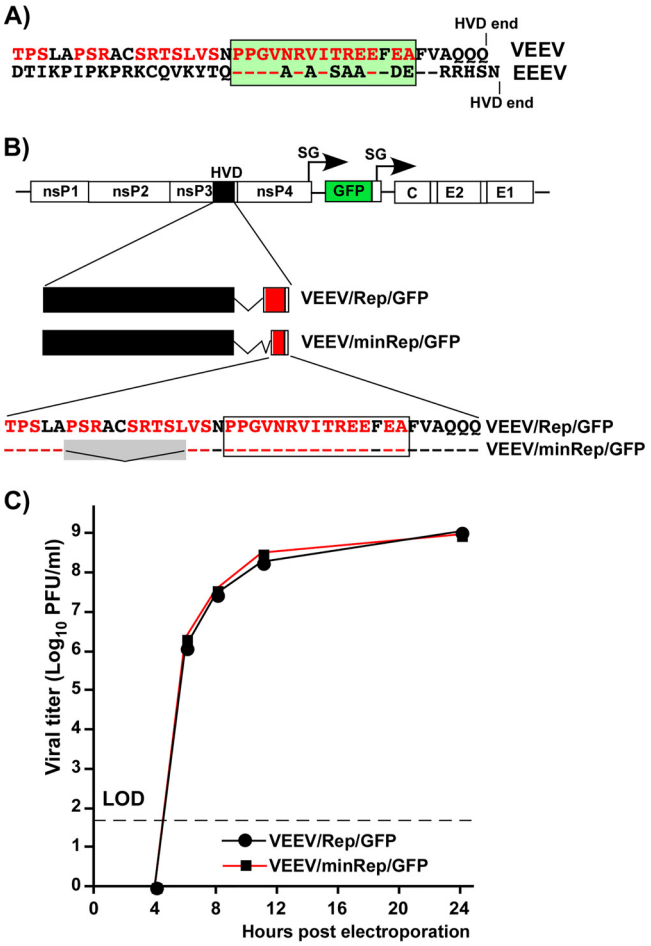

FIG 3 The C-terminal element of the repeat in VEEV nsP3 HVD can be shortened without a negative effect on viral replication. (A) Alignment of the amino acid sequences of the very C-terminal element of the repeat in VEEV/Rep/GFP (indicated in red) and the FXR-binding sequence in the C terminus of EEEV HVD. Identical amino acids are shown by dashed lines. The box indicates putative common FXR-binding sequences. (B) Schematic presentation of the viral genome, mutated HVDs, and amino acid sequences of the FXR-binding peptides in VEEV/Rep/GFP and VEEV/minRep/GFP. Black boxes indicate fragments derived from artHVD. Red boxes indicate the residual element of the repeat. Dashed lines indicate identical amino acids. The gray box indicates deleted amino acids. (C) BHK-21 cells were electroporated with 3 μg of the *in vitro*-synthesized RNAs. Viral samples were collected at the indicated time points, and titers were determined by a plaque assay on BHK-21 cells. LOD indicates the limit of detection. The experiment was performed twice, and no difference in replication rates between these viruses was detected. Data from one of the experiments are presented.

domains or the nsP3 macrodomain. They were cloned back into the genomes of the original deletion mutants (Fig. 5A). Equal amounts of the *in vitro*-synthesized RNAs of the parental mutants and their derivatives with identified mutations were electroporated into BHK-21 cells, and viral titers were assessed at 24 h postelectroporation. The introduced nsP2- and nsP3-specific mutations had strong positive impacts on viral replication (Fig. 5B). However, their effects on RNA infectivities in the ICA were statistically insignificant (data not shown). The infectivities remained like those of parental deletion mutants and 10-fold below the level demonstrated by the *in vitro*-synthesized RNA of VEEV/GFP (Fig. 4B). This was an indication that in the *in vitro* experiments, the introduced compensatory mutations likely had no positive effects on the initiation of replication of the G RNAs encoding a defective HVD repeat but were able to increase the rates of RNA synthesis after replication had already been established.

VEEV variants that lack FXR- or SH3 domain-binding motifs can replicate in a variety of cell lines. In previous studies, we found that BHK-21 cells are exceptionally

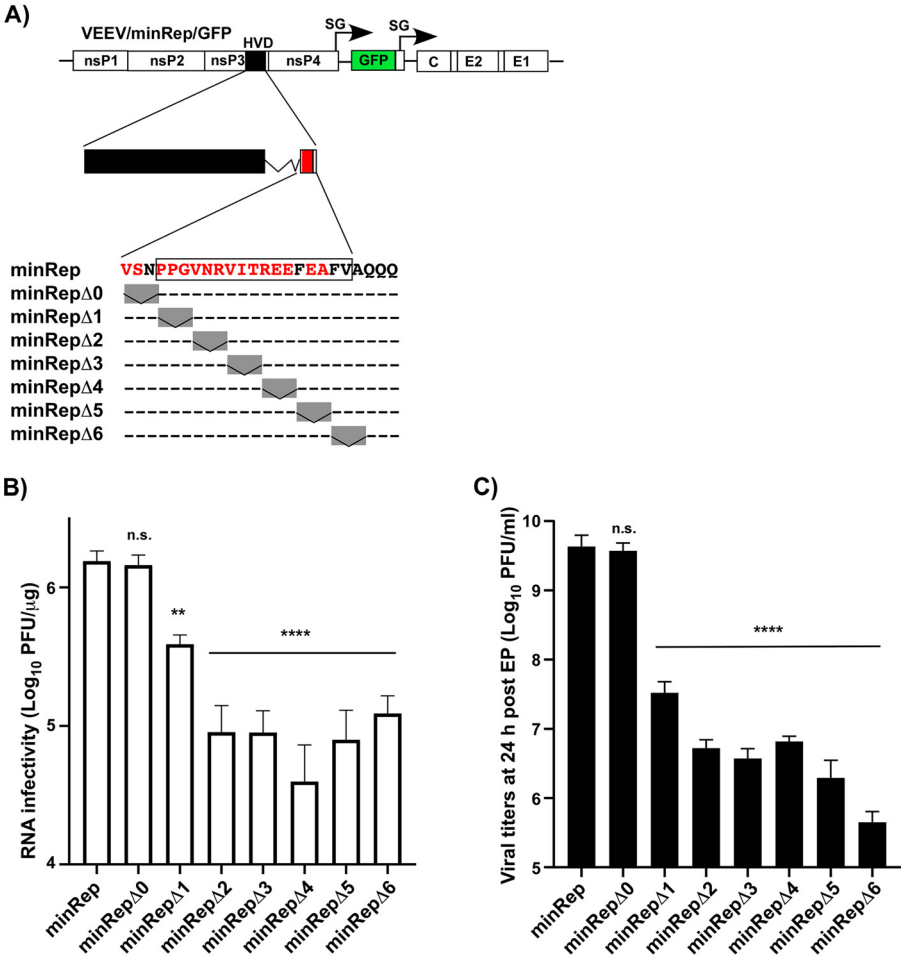

FIG 4 Small deletions in the minimal FXR-binding motif have deleterious effects on VEEV replication. (A) Schematic presentation of the VEEV/minRep/GFP genome, its HVD, and deletions introduced into the minRep sequence. The black box indicates a mutated HVD derived from artHVD. The red box indicates the position of the minimized element of the repeat. Dashed lines indicate identical amino acids. Gray boxes indicate positions of the deletions. (B) BHK-21 cells were electroporated with 3 μg of the *in vitro*-synthesized RNAs, and these cells were used to assess RNA infectivity in an ICA (see Materials and Methods for details). (C) The rest of the electroporated cells were seeded into 100-mm dishes. Media were harvested at 24 h postelectroporation (post EP), and viral titers were determined by a plaque assay on BHK-21 cells. The experiments were performed 2 times and demonstrated very similar differences. Significances of differences among the values were determined by one-way analysis of variance (ANOVA), followed by Dunnett's multiple-comparison test (n.s., not significant; **, $P < 0.01$; ****, $P < 0.0001$). Data are presented as means with standard deviations (SD) ($n = 3$).

efficient in supporting replication of alphavirus mutants with severely altered functions of nsP3 and nsP2 (27). The same mutants or their second-site revertants (pseudorevertants) could be nonviable or very poorly replicating in other cell types (27, 41). Therefore, we next compared the efficiencies of VEEV/GFP, VEEV/minRep/GFP, and VEEV/ΔRep/GFP replication in MRC-5 (human), NIH 3T3 (murine), BHK-21 (hamster), and C7/10 (mosquito) cells. These cell lines were infected with VEEV mutants at the same MOI, and titers of the released viruses were assessed 8 and 24 h after infection of vertebrate cells and 20 and 48 h after infection of C7/10 cells (Fig. 6). As we expected, HVD mutants demonstrated the most efficient replication in the BHK-21 cell line. Compared to parental VEEV/GFP, the lack of HVD repeats in VEEV/ΔRep/GFP had a stronger negative effect on virus release from human and mosquito cells than from BHK-21 and NIH 3T3 cells. The replication of VEEV/minRep/GFP, which contained a single minimal FXR-binding element of the repeat in the context of artHVD, was less affected in the vertebrate cells used. However, in C7/10 cells at 48 h p.i., this mutant accumulated in the medium to >100-fold-lower titers (Fig. 6).

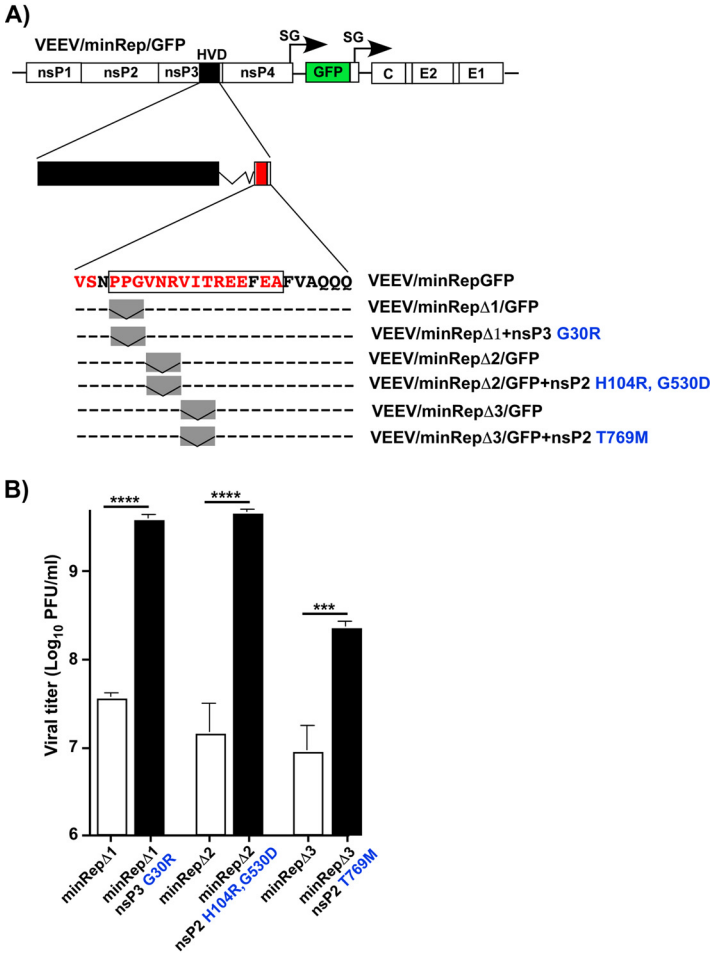

FIG 5 The identified adaptive mutations in nsP3 and nsP2 have positive effects on the replication of VEEV with a mutated HVD. (A) Schematic presentation of the VEEV/minRep/GFP genome, its HVD, and deletions in the minRep sequence and the corresponding evolved variants. Mutations identified in the plaque isolates and cloned into the genomes of the corresponding parental viruses are indicated in blue. (B) BHK-21 cells were electroporated with 3 μg of the *in vitro*-synthesized RNAs of the indicated mutants, and media were harvested at 24 h posttransfection. Viral titers were determined by a plaque assay on BHK-21 cells. Significances of differences among the values were determined by a two-tailed unpaired *t* test (***, $P < 0.001$; ****, $P < 0.0001$). Data are presented as means with SD ($n = 3$).

Interestingly, in Vero cells, VEEV/ΔRep/GFP demonstrated essentially no replication (Fig. 7A). Since Vero cells are very susceptible to the replication of wt VEEV TC-83 that has an unmodified HVD (42), we evaluated the levels of CD2AP, SH3KBP1, and another SH3 domain-containing protein, BIN1, in this cell line. The expression of BIN1 was evaluated because this protein was found to interact with HVDs of other alphaviruses (31, 33). Compared to MRC-5 (Fig. 7B) and other cell lines (40), all the isoforms of the indicated proteins were present in Vero cells at very low concentrations (Fig. 7B). HVD of the VEEV/ΔRep/GFP mutant does not contain the FXR-binding motif, which could drive interactions with FXR family members and subsequent RC formation. In Vero cells, this inability may be not compensated for by interactions with the SH3 domain-containing cellular proteins that were able to support to some extent VEEV RNA replication in other cells (Fig. 6). However, the role of other possible genetic defects in Vero cells cannot be ruled out. Interestingly, attempts to generate stable Vero cell lines expressing higher levels of CD2AP or SH3KBP1 were unsuccessful, and the indicated ectopically expressed fusions of these proteins with Cherry were rapidly degrading (data not shown).

Thus, the results of these experiments demonstrated that (i) the designed VEEV/minRep/GFP and VEEV/ΔRep/GFP mutants are viable in most of the tested cell lines; (ii)

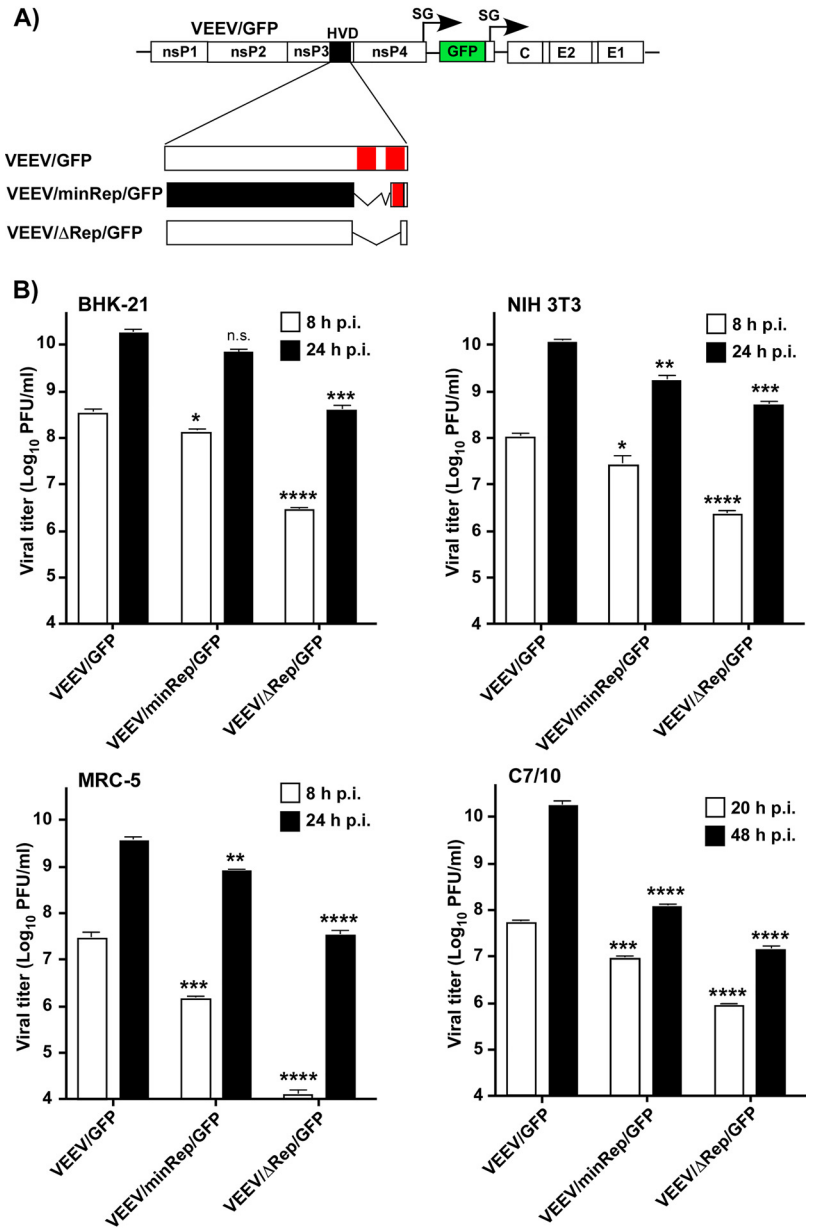

FIG 6 The designed FXR- or SH3-dependent VEEV mutants retain the ability to replicate in a variety of cell lines. (A) Schematic presentation of the viral genome and the designed mutated HVDs. Open boxes indicate wt amino acid sequences. The black box indicates a mutated, artHVD-derived fragment. Positions of FXR-binding elements are shown by red boxes. (B) The indicated cell lines were infected with VEEV/GFP and the designed mutants at an MOI of 1 PFU/cell, and titers of the released viruses were assessed at 8 and 24 h p.i. by a plaque assay on BHK-21 cells. Significances of differences between VEEV and mutants at different time points were determined by one-way ANOVA, followed by Dunnett's multiple-comparison test (n.s., not significant; *, $P < 0.1$; **, $P < 0.01$; ***, $P < 0.001$; ****, $P < 0.0001$). Data are presented as means with SD ($n = 3$).

the C-terminal FXR-binding motif of VEEV HVD plays a critical role(s) in viral replication in the tested vertebrate and mosquito cells; and (iii) the rest of HVD, which contains the SH3 domain-binding motif(s), appears to play a redundant role in VEEV replication and is more important for viral replication in mosquito C7/10 cells.

Effects of modifications of HVD on VEEV pathogenesis. For the *in vivo* experiments, we applied (i) the above-described VEEV variant that encodes no FXR-binding repeats in the HVD (VEEV/ΔRep/GFP), (ii) VEEV that encodes a single minimal FXR-binding element of the repeat and has the rest of HVD mutated (VEEV/minRep/GFP),

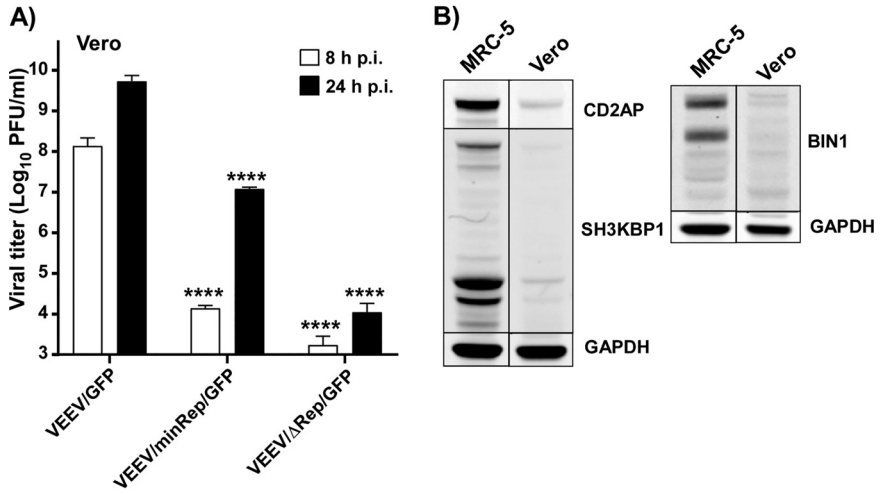

FIG 7 Vero cells support the replication of the VEEV/ΔRep/GFP mutant very inefficiently. (A) Subconfluent Vero cells in 6-well Costar plates were infected with the indicated VEEV variants at an MOI of 1 PFU/cell, and titers of the released viruses were assessed at 8 and 24 h p.i. by a plaque assay on BHK-21 cells. Differences between VEEV and mutants at different time points had *P* values of <0.0001, as determined by one-way ANOVA followed by Dunnett's multiple-comparison test (****, $P < 0.0001$). Data are presented as means with SD ($n = 3$). (B) The presence of CD2AP, SH3KBP1, and BIN1 in MRC-5 and Vero cells was analyzed by Western blotting using the indicated primary and corresponding secondary Abs. Membranes were scanned on a Li-Cor imager. GAPDH, glyceraldehyde-3-phosphate dehydrogenase.

and (iii) the parental VEEV/GFP. In addition, previous studies demonstrated that VEEV TC-83 can tolerate a replacement of the entire natural HVD by those derived from SINV and CHIKV (31, 41). These VEEV mutants with heterologous HVDs were capable of efficient replication despite utilizing different host factors in RC formation and function. Therefore, we included in experiments another VEEV mutant, VEEV/chikvHVD/GFP, which encoded a 185-aa-long fragment of the CHIKV HVD instead of the natural VEEV-specific counterpart (Fig. 8A). Thus, the replication of the chimeric virus was expected to become dependent on interactions with G3BPs but not with FXR family members.

Six-day-old CD1 mice were subcutaneously (s.c.) infected with 2×10^5 PFU of VEEV/GFP or the indicated nsP3 HVD mutants to compare levels of viremia, viral titers in the brains, survival, weight gain, and titers of induced neutralizing Abs (Fig. 8B). On day 1 p.i., all of the designed viruses induced readily detectable viremia, and by day 5 p.i., viremia became either undetectable or close to the limit of detection. VEEV/chikvHVD/GFP replicated in the brains of suckling mice to titers similar to those of VEEV/GFP and caused strong delays in weight gain, suggesting severity of the disease. However, in contrast to parental VEEV/GFP, more than 60% of mice survived the infection, indicating the negative effect of HVD replacement on virulence. The presence of a single minimal FXR-binding element of the repeat in the artificial HVD decreased the rates of VEEV/minRep/GFP accumulation in mouse brains, but by day 5 p.i., brain titers of the virus approached 10^9 PFU/g. They also correlated with delays in gaining weight. Nevertheless, despite strong signs of the disease, all of the mice remained alive and eventually recovered. VEEV/ΔRep/GFP demonstrated the best performance in terms of viral attenuation. Compared to VEEV/GFP, at day 5 p.i., this mutant was detected in the brains at concentrations that were 6 orders of magnitude lower, if at all. Mice exhibited no signs of the disease and were gaining weight as efficiently as the uninfected group, and all of them survived the infection. Thus, the deletion of both repeats made the resulting VEEV/ΔRep/GFP dramatically less neuroinvasive and likely less neurovirulent for suckling mice.

All the surviving mice, including those infected with VEEV/ΔRep/GFP, responded to infections with high titers of neutralizing Abs (Fig. 8B), which were not significantly different between the groups. Taken together, these results suggested that manipula-

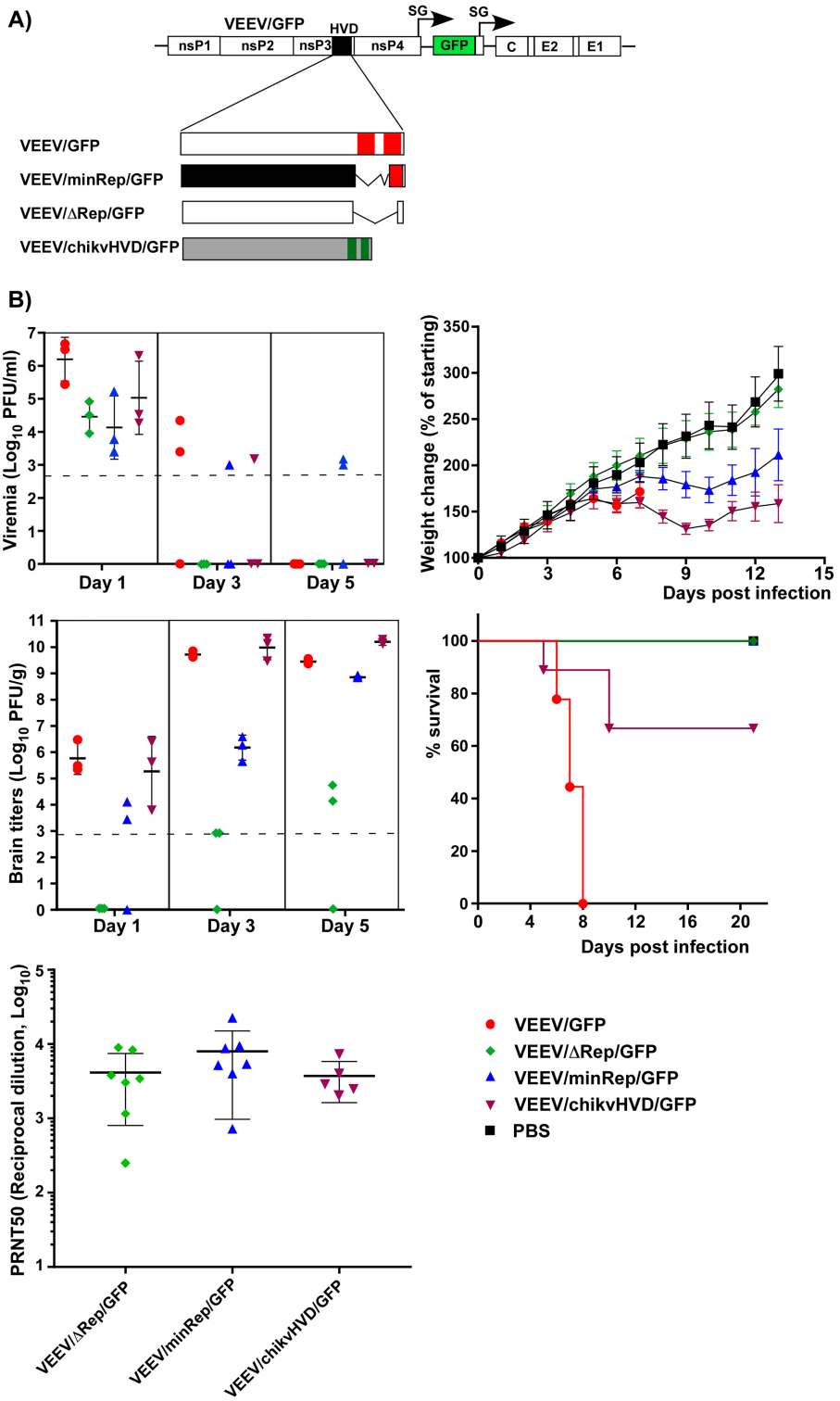

FIG 8 Modifications of HVD affect the pathogenesis of VEEV TC-83-based constructs in suckling mice. (A) Schematic presentation of HVDs encoded by recombinant viral genomes. Open boxes indicate wt amino acid sequences; the black box indicates a mutated, artHVD-derived fragment; and the gray box indicates CHIKV HVD. VEEV repeats are shown in red, and CHIKV-specific, G3BP-binding repeats are shown in green. (B) Six-day-old mice were infected s.c. with 2×10^5 PFU of the indicated VEEV HVD mutants or parental VEEV/GFP. Panels show the levels of viremia and brain titers (means with standard deviations where applicable), weight changes (means with standard deviations), survival, and titers of neutralizing Abs at day 21 p.i. (means with standard deviations) in surviving mice. Viral titers were assessed by a plaque assay on BHK-21 cells. The dashed lines indicate the limits of detection.

tions with nsP3 additionally contributed to VEEV TC-83 attenuation, which, in this strain, is determined by mutations in the 5′ untranslated region (UTR) and E2 glycoprotein (7, 43–46).

The second group of VEEV HVD mutants was designed based on the enzootic strain VEEV ZPC738 (wVEEV) (Fig. 9A). Similar to the VEEV TC-83-based construct, wVEEV/minRep encoded an artificially designed HVD with only a single FXR-binding site and with the rest of the HVD randomized. wVEEV/ΔRep had the FXR-binding repeat deleted, and wVEEV/chikvHVDdel1 had the natural VEEV HVD replaced by the CHIKV-specific counterpart. Since in the above-described experiments in suckling mice (Fig. 8), the TC-83-based construct VEEV/chikvHVD/GFP did not demonstrate advanced attenuation and remained neurovirulent, the CHIKV HVD fragment was additionally modified. We deleted the first G3BP-binding motif in the CHIKV-specific sequence. All of the designed constructs, including the parental wVEEV, were rescued in biosafety level 3 (BSL3) containment, and adult 4- to 5-week-old CD1 mice were then infected s.c. with 1×10^3 PFU of each variant.

The parental wVEEV was universally lethal for all of the infected mice. They succumbed to the infection within 6 days (Fig. 9B). Despite strong modifications in the HVD, wVEEV/ΔRep, wVEEV/minRep, and wVEEV/chikvHVDdel1 developed viremia at day 1 p.i. and remained neuroinvasive (Fig. 9B). The differences in the levels of induced viremia were particularly evident at day 3 p.i. However, all the mutants were able to replicate in the brains of adult mice to the titers comparable to those of the parental wVEEV. The infected mice were losing weight, and those that received wVEEV/minRep died within 8 days p.i. Thus, the presence of even a single element of the FXR-binding repeat in the absence of all other motifs was sufficient for supporting the lethal phenotype of enzootic VEEV ZPC738-based virus. wVEEV/ΔRep was more attenuated, but surprisingly, the effect of the deletion of the C-terminal repeat was not as strong as that detected for the similar TC-83-based VEEV/ΔRep/GFP construct in suckling mice. Nevertheless, despite virus replication in the brain and severe weight loss, about 30% of mice survived the infection. None of the mice infected with the designed wVEEV/chikvHVDdel1 died, indicating its strong attenuation compared to other HVD mutants.

Taken together, the results of experiments with HVD mutants in VEEV TC-83 and ZPC738 backgrounds demonstrated that modifications of HVD have a negative effect on viral pathogenesis. However, they do not eliminate neuroinvasiveness and, if introduced alone, are insufficient for preventing both viral entry and replication in the brain.

DISCUSSION

Among alphavirus nonstructural proteins, functions of nsP3 are the least understood. This protein appears to be not directly involved in the synthesis of virus-specific RNAs but is indispensable for viral replication. The mutations in the conserved N-terminal macrodomain and the following AUD affect the efficiency of SG RNA synthesis (26), mono-ADP-ribosylhydrolase activity (18, 20–22), inhibition of cellular translation (23), and viral pathogenesis (22). In contrast to the macrodomain and AUD, the C-terminal domains, HVDs, of different alphaviruses are predicted, and experimentally demonstrated in the case of CHIKV (34), to be intrinsically disordered (1, 40). They also exhibit essentially no identity at the amino acid level (1). The accumulating experimental data strongly suggest that despite very high levels of variations in amino acid sequence and length, alphavirus HVDs have common features, which are critical determinants of viral replication in both vertebrate and mosquito cells. Alphavirus HVDs contain multiple short linear motifs that interact with host factors, which are required for RC assembly and function (33–36). In all of the alphaviruses studied to date, the C-terminal HVD fragments contain short, often repeating peptides that mediate interactions with the most critical host factors, such as G3BP/Rasputin and/or FXR family members (31, 39, 47). The HVD fragments located upstream of the repeats contain proline-rich sequences that can interact with multiple SH3 domain-containing proteins of mammalian and mosquito cells (34, 35, 48, 49).

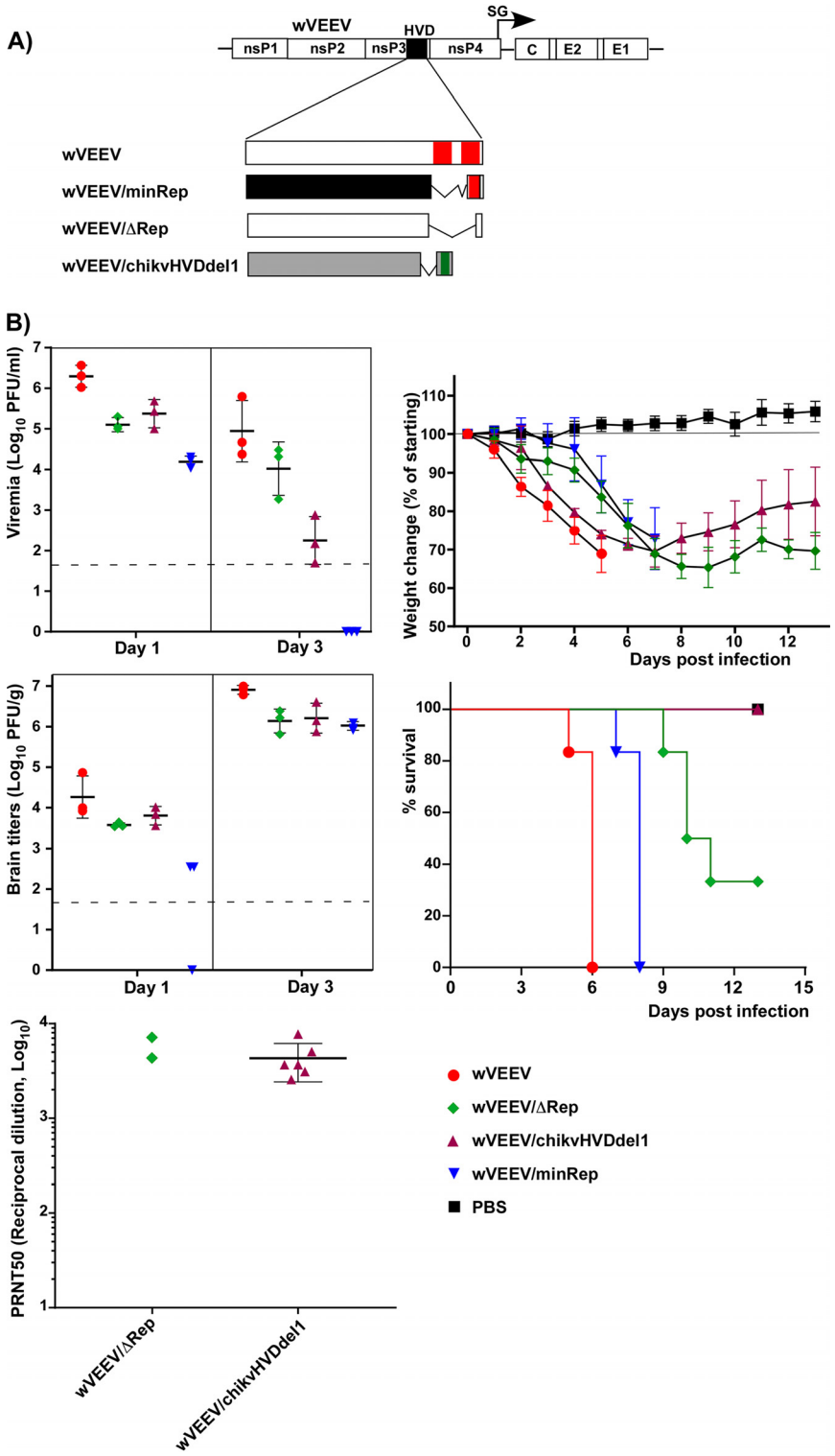

FIG 9 Modifications of HVD in wVEEV (VEEV ZPC738) differentially affect viral pathogenesis in adult mice. (A) Schematic presentation of HVDs encoded by recombinant viral genomes. Open boxes indicate wt amino acid sequences; the black box indicates a mutated, artHVD-derived fragment; and the gray box indicates CHIKV HVD. VEEV repeats are shown in red, and the CHIKV-specific element of G3BP-binding repeats is shown in green. (B) Four- to five-week-old CD1 mice were infected s.c. with 1×10^3 PFU of each indicated viral variant. Panels show the levels of viremia and brain titers (means with standard deviations where applicable), weight changes (means with standard deviations), survival, and titers of neutralizing Abs measured at day 18 p.i. (means with standard deviations) in surviving mice. Viral titers were assessed by a plaque assay on BHK-21 cells. The dashed lines indicate the limits of detection.

In OW alphavirus infections, the very C-terminal, repeating HVD elements interact with both members of the G3BP family (39). In mosquito cells, the same repeats bind the insect homolog of G3BP, Rasputin (Rin1) (47). Interestingly, the insect-specific alphavirus Eilat virus (EILV) encodes the same HVD repeat as that found in viruses capable of replication in vertebrate cells (50, 51). This is an additional indication of the importance and conservation of this interaction in alphavirus evolution. Moreover, the HVD of the NW alphavirus EEEV has acquired a G3BP-binding motif (33). Its sequence is very different from that found in the C-terminal repeat in the HVDs of the OW alphaviruses, but it supports interactions with G3BPs and EEEV replication in G3BP-expressing cells (33).

In contrast to the OW alphaviruses (SFV, SINV, and EILV), the C-terminal HVD of the NW alphavirus VEEV does not interact with G3BPs but instead binds all three members of the FXR protein family (31, 33, 41). The data from our previous study (27) and this study suggested that the HVD-FXR interaction is mediated by the 33-aa-long repeat located in the C terminus of VEEV nsP3 HVD. Our new data demonstrate that in this repeat, the functional sequence is relatively short and is similar to the FXR-binding motif that we have previously described for EEEV HVD (33). The presence of this minimal peptide alone in the strongly mutated HVD is sufficient for driving VEEV replication (Fig. 3), and VEEV ZPC738-based virus (wVEEV/minRep) remains neurovirulent in a mouse model. Small deletions in the minimal FXR-binding motif of VEE/minRep/GFP have a deleterious effect on viral replication. Such deletion mutants are essentially nonviable unless they acquire compensatory mutations in nsP2 and/or nsP3 (Fig. 4 and 5). Thus, the FXR-binding motif is one of the key contributors to VEEV replication and, ultimately, pathogenesis. Importantly, the identified minimal peptide is not absolutely conserved among the NW alphaviruses. In the EEEV-specific FXR-binding peptide, 7 aa are different from those in the VEEV-specific counterpart (Fig. 3A). To date, it remains unclear why in natural isolates of VEEV the conserved FXR-binding peptide is longer than the identified minimal interacting sequence. Moreover, based on GenBank data, some of the viruses in the VEEV serocomplex contain a single motif, and others contain it in two copies (27). One of the possible explanations is that the acquisition of the FXR-binding peptide by VEEV was a relatively recent event in viral evolution and that the amino acid sequence has not yet been minimized.

Other results of this study unambiguously demonstrate that FXR-HVD binding is not the only determinant of VEEV replication. The SH3 domain-containing proteins were found to strongly interact with the motif(s) located between aa 391 and 465 of VEEV nsP3 in the middle of its HVD, and an additional relatively weak interaction was detected with the downstream-located HVD fragment (Fig. 1). The HVD interaction with SH3 domain-containing proteins was found to be sufficient for supporting the replication of VEEV/ΔRep/GFP, which has no FXR-binding motifs in its HVD (Fig. 2). However, its replication was less efficient than those of VEEV/GFP and VEEV/minRep/GFP, which utilize the FXR-HVD interaction in RC assembly and function. In good correlation with the *in vitro* data, VEEV/ΔRep/GFP became dramatically less pathogenic for suckling mice (Fig. 8). Surprisingly, a similar ΔRep variant of VEEV ZPC738 remained pathogenic for adult mice (Fig. 9). Thus, the SH3 domain-binding motifs are also important determinants of VEEV replication and pathogenesis, supporting the hypothesis that the redundant use of cellular host factors allows viral replication in multiple tissues where expression can vary. However, their function also depends on the virus genetic background.

Importantly, other results of the analysis of nsP3 HVD structure and function demonstrate that the entire natural VEEV HVD can be replaced by the CHIKV- or SINV-derived counterpart without profound negative effects on viral replication *in vitro* (31, 41). In this study, VEEV/chikvHVD/GFP remained lethal for suckling mice, and despite lacking one of the G3BP-binding sites, wVEEV/chikvHVDdel1 induced readily detectable disease in adult mice (Fig. 8 and 9). Thus, the NW alphavirus VEEV is capable of replication using a G3BP-dependent mechanism. On the other hand, the reciprocal replacement of HVD in CHIKV with the VEEV counterpart makes chimeric CHIKV

nonviable (31). This suggests that SH3 domain-containing proteins and FXRs in particular, which bind to the VEEV HVD, are insufficient for supporting CHIKV replication. Alternatively, there are additional interactions of G3BP with other cellular or/and viral proteins that are important for CHIKV RC formation and function, but they remain to be discovered. It is also possible that although VEEV apparently lost the G3BP-binding motifs during its evolution and became capable of using FXRs, it has retained an ability to utilize G3BP in RC function if the corresponding motifs are cloned back into its HVD.

It was tempting to expect that manipulations with VEEV HVD could be used as a means of viral attenuation to make it less neurovirulent. The results of this study suggest that HVD-specific changes certainly can be applied but not alone. wVEEV variants with mutated HVD remained neuroinvasive and neurovirulent in adult mice. However, the same mutants in the VEEV TC-83 background, particularly VEEV/ΔRep/GFP, can be less pathogenic than the parental virus. Thus, modifications in HVD need to be applied in combination with attenuating mutations in either glycoproteins and the 5′ UTR, which were acquired by serial VEEV passage (52, 53), or capsid protein (54–56) and/or the packaging signal (57). The mutations in the capsid nuclear localization signal (NLS) and the 5′ UTR make VEEV a potent type I interferon (IFN) inducer and more sensitive to one of the interferon-stimulated genes, IFIT1, respectively (44, 58, 59). An additional complication in the application of HVD-specific mutations is that they directly affect viral replication rates. This defect, in turn, opens an opportunity for viral evolution to a more efficiently replicating phenotype by acquiring adaptive mutations in the nsPs (60, 61). Such evolution has been detected in the experiments with VEEV/artHVD/GFP and other mutants, and it is unlikely that it can be eliminated.

In summary, the results of this study demonstrate that (i) VEEV is fundamentally different from CHIKV in terms of the assembly and function of HVD-specific protein complexes; (ii) in contrast to CHIKV, either FXRs or SH3 domain-containing cellular proteins can support VEEV replication albeit with different efficiencies; (iii) FXR-binding peptides are located at the C terminus of VEEV HVD; (iv) the minimal FXR-binding site is 15 aa long and exhibits a high level of identity with that of EEEV; (v) the binding site(s) of the SH3 domain-containing proteins in the HVD is located between aa 391 and 465 of VEEV nsP3, with an additional, weak binding site located in the downstream amino acid sequence; (vi) the effects of modifications of VEEV HVD on viral pathogenesis depend on mouse age and the genetic background of the virus; and (vii) manipulations with VEEV HVD, including its replacement with its CHIKV-specific counterpart, can be used for viral attenuation but only if they are applied in combination with other modifications that alter viral cell specificity and/or the ability to interfere with the innate immune response.

MATERIALS AND METHODS

Cell cultures. BHK-21 cells were kindly provided by Paul Olivo (Washington University, St. Louis, MO). NIH 3T3, MRC-5, HFF-1, HEK 293, and Vero cells were obtained from the American Type Culture Collection (Manassas, VA). BHK-21, NIH 3T3, HEK 293, and Vero cells were maintained in alpha minimum essential medium supplemented with 10% fetal bovine serum (FBS) and vitamins. MRC-5 cells were maintained in Dulbecco's modified Eagle medium (DMEM) supplemented with 10% FBS. C7/10 cells were provided by Henry Huang (Washington University, St. Louis, MO). They were maintained in DMEM supplemented with 10% FBS and 10% tryptose phosphate broth (TPB) at 28°C with 5% CO_2.

Plasmid constructs. A plasmid encoding infectious cDNA of VEEV TC-83, pVEEV/GFP, was described previously (58). A plasmid encoding wt VEEV ZPC738 (62) was provided by Scott Weaver (University of Texas Medical Branch at Galveston, TX). For this study, the original T7 promoter was replaced by the SP6 promoter. All of the modifications in the HVDs encoded by cDNAs of both plasmids were made by using standard PCR-based techniques. To simplify the presentation of data in the text, all the constructs based on the VEEV TC-83 genome were labeled VEEV, and those based on VEEV ZPC738 were labeled wVEEV. Plasmids containing cDNA of the SINV replicon have been described previously (63). They encoded the SINV genome with all of the structural genes replaced by heterologous sequences. DNA sequences encoding different variants of Flag-GFP-HVDveev were also designed by PCR and cloned into cDNA of the SINV replicon under the control of the SG RNA promoter using standard recombinant DNA techniques. All of the constructs are schematically presented in the corresponding figures. The cDNA of the SINV helper genome used had the fragment encoding viral nsPs deleted, and it retained the subgenomic promoter and all of the viral structural genes (64). Nucleotide sequences of the plasmids are available upon request.

RNA transcriptions, RNA infectivity assay, and rescue of recombinant viruses. Plasmids containing viral, replicon, and helper genomes were purified by ultracentrifugation in CsCl gradients. They were linearized in restriction sites located downstream of the poly(A) tails. RNAs were synthesized *in vitro* by using SP6 RNA polymerase (Invitrogen) in the presence of a cap analog (New England BioLabs) according to recommendations of the manufacturers. The quality and yields of the transcripts were analyzed by agarose gel electrophoresis. Aliquots of the reaction mixtures were used for electroporation of BHK-21 cells under conditions described previously (65, 66). For packaging of SINV replicons into infectious viral particles, their RNAs were mixed with the *in vitro*-synthesized helper RNA (64) and used for electroporation. Viruses and packaged replicons were harvested at 24 h postelectroporation. Viral titers were determined by a plaque assay on BHK-21 cells (67). Titers of the packaged replicons were determined by infecting 5×10^5 BHK-21 cells in 6-well Costar plates by serial 10-fold dilutions of the stocks. At 6 h p.i., titers were determined by evaluating the percentage of GFP-positive cells at appropriate dilutions.

Infectivities of the *in vitro*-synthesized G RNAs were analyzed by an infectious center assay (ICA). Tenfold dilutions of electroporated BHK-21 cells were seeded into 6-well Costar plates with monolayers of naive BHK-21 cells. After 2 h of incubation at 37°C, they were covered with 0.5% agarose supplemented with DMEM and 3% FBS. Plaques were stained with crystal violet at 2 days postelectroporation. RNA infectivities were determined as PFU per microgram of electroporated RNAs.

Coimmunoprecipitation. NIH 3T3 and HEK 293 cells were infected with packaged SINV replicons at an MOI of 20 inf.u/cell. At ~3 h p.i., when GFP expression just became detectable under a fluorescence microscope, cells were harvested, and their lysates were prepared for immunoprecipitation as previously described (30). The postnuclear supernatants were incubated with magnetic beads with anti-Flag Abs. Protein complexes were analyzed by Western blotting using anti-CD2AP rabbit polyclonal antibodies (catalog number sc-9137; Santa Cruz Biotechnology), anti-SH3KBP1 mouse monoclonal antibodies (catalog number sc-166862; Santa Cruz Biotechnology), anti-FXR1 rabbit monoclonal antibodies (catalog number 12295; Cell Signaling), and anti-Flag mouse monoclonal antibodies (catalog number F1804; Sigma). After incubation with the corresponding infrared dye-labeled secondary Abs, membranes were scanned on a Li-Cor imager.

Animal studies. To evaluate the ability of candidate viruses to develop viremia and invade and replicate in brains, 6-day-old CD1 mice were inoculated s.c. with 2×10^5 PFU of the designed VEEV TC-83-based viruses in 20 μl of phosphate-buffered saline (PBS) supplemented with 1% mouse serum. At 1, 3, and 5 days p.i., mice were sacrificed, and viral titers in the blood and in the brain were assessed by a plaque assay on BHK-21 cells. At 21 days p.i., sera were analyzed for the levels of neutralizing Abs.

Adult 4- to 5-week-old CD1 mice were inoculated s.c. with 1×10^3 PFU of ZPC738-based VEEV variants diluted in PBS containing 1% mouse serum. Animals were monitored daily for weight changes and signs of disease. At the times p.i. indicated in the figures, animals were sacrificed, and blood and brain samples were collected and analyzed for either viremia or levels of neutralizing Abs. All the animal studies were carried out under the approval of the Institutional Animal Care and Use Committee of the University of Alabama at Birmingham (UAB). The experiments with VEEV TC-83- and ZPC738 (wVEEV)-based mutants were carried out in animal biosafety level 2 (ABSL2) and ABSL3 facilities, respectively. All the mice were sacrificed humanely after the completion of the study.

Neutralizing antibody titers (50% plaque reduction/neutralization titer [$PRNT_{50}$]). Serum samples were incubated at 50°C for 1 h and then serially diluted in PBS supplemented with 1% FBS and 250 PFU/ml of VEEV TC-83. Samples were incubated at 37°C for 2 h, and aliquots were then applied to monolayers of BHK-21 cells in 6-well Costar plates. After incubation at 37°C for 1 h, the cells were overlaid with 0.5% agarose supplemented with DMEM and 3% FBS. After 2 days of incubation, plaques were stained with crystal violet. The percentage of reduction was calculated using GraphPad Prism software.

ACKNOWLEDGMENTS

We thank Scott Weaver for providing the infectious cDNA clone of CHIKV 181/25. We also thank Valeriya Kuznetsova for technical assistance.

This study was supported by Public Health Service grants R01AI133159 and R01AI118867 to E.I.F. and R01AI095449 to I.F.

REFERENCES

1. Strauss JH, Strauss EG. 1994. The alphaviruses: gene expression, replication, evolution. Microbiol Rev 58:491–562.
2. Weaver SC. 2001. Venezuelan equine encephalitis, p 539–548. *In* Service MW (ed), The encyclopedia of arthropod-transmitted infections. CAB International, Wallingford, United Kingdom.
3. Weaver SC. 2001. Eastern equine encephalitis, p 151–159. *In* Service MW (ed), The encyclopedia of arthropod-transmitted infections. CAB International, Wallingford, United Kingdom.
4. Weaver SC, Frolov I. 2005. Togaviruses, p 1010–1024. *In* Mahy BWJ, ter Meulen V (ed), Virology, vol 2. Hodder Arnold, Salisbury, United Kingdom.
5. Bronze MS, Huycke MM, Machado LJ, Voskuhl GW, Greenfield RA. 2002. Viral agents as biological weapons and agents of bioterrorism. Am J Med Sci 323:316–325. https://doi.org/10.1097/00000441-200206000-00004.
6. Kinney RM, Johnson BJ, Welch JB, Tsuchiya KR, Trent DW. 1989. The full-length nucleotide sequences of the virulent Trinidad donkey strain of Venezuelan equine encephalitis virus and its attenuated vaccine derivative, strain TC-83. Virology 170:19–30. https://doi.org/10.1016/0042-6822(89)90347-4.
7. Kinney RM, Chang GJ, Tsuchiya KR, Sneider JM, Roehrig JT, Woodward TM, Trent DW. 1993. Attenuation of Venezuelan equine encephalitis virus strain TC-83 is encoded by the 5′-noncoding region and the E2 envelope glycoprotein. J Virol 67:1269–1277.
8. Strauss EG, Rice CM, Strauss JH. 1984. Complete nucleotide sequence of

the genomic RNA of Sindbis virus. Virology 133:92–110. https://doi.org/10.1016/0042-6822(84)90428-8.
9. Rupp JC, Sokoloski KJ, Gebhart NN, Hardy RW. 2015. Alphavirus RNA synthesis and non-structural protein functions. J Gen Virol 96:2483–2500. https://doi.org/10.1099/jgv.0.000249.
10. Ahola T, Kaariainen L. 1995. Reaction in alphavirus mRNA capping: formation of a covalent complex of nonstructural protein nsP1 with 7-methyl-GMP. Proc Natl Acad Sci U S A 92:507–511. https://doi.org/10.1073/pnas.92.2.507.
11. Vasiljeva L, Merits A, Auvinen P, Kaariainen L. 2000. Identification of a novel function of the alphavirus capping apparatus. RNA 5′-triphosphatase activity of Nsp2. J Biol Chem 275:17281–17287. https://doi.org/10.1074/jbc.M910340199.
12. Rubach JK, Wasik BR, Rupp JC, Kuhn RJ, Hardy RW, Smith JL. 2009. Characterization of purified Sindbis virus nsP4 RNA-dependent RNA polymerase activity in vitro. Virology 384:201–208. https://doi.org/10.1016/j.virol.2008.10.030.
13. Rupp JC, Jundt N, Hardy RW. 2011. Requirement for the amino-terminal domain of Sindbis virus nsP4 during virus infection. J Virol 85:3449–3460. https://doi.org/10.1128/JVI.02058-10.
14. Russo AT, White MA, Watowich SJ. 2006. The crystal structure of the Venezuelan equine encephalitis alphavirus nsP2 protease. Structure 14:1449–1458. https://doi.org/10.1016/j.str.2006.07.010.
15. Stapleford KA, Rozen-Gagnon K, Das PK, Saul S, Poirier EZ, Blanc H, Vidalain PO, Merits A, Vignuzzi M. 2015. Viral polymerase-helicase complexes regulate replication fidelity to overcome intracellular nucleotide depletion. J Virol 89:11233–11244. https://doi.org/10.1128/JVI.01553-15.
16. Tomar S, Hardy RW, Smith JL, Kuhn RJ. 2006. Catalytic core of alphavirus nonstructural protein nsP4 possesses terminal adenylyltransferase activity. J Virol 80:9962–9969. https://doi.org/10.1128/JVI.01067-06.
17. Law YS, Utt A, Tan YB, Zheng J, Wang S, Chen MW, Griffin PR, Merits A, Luo D. 2019. Structural insights into RNA recognition by the chikungunya virus nsP2 helicase. Proc Natl Acad Sci U S A 116:9558–9567. https://doi.org/10.1073/pnas.1900656116.
18. Malet H, Coutard B, Jamal S, Dutartre H, Papageorgiou N, Neuvonen M, Ahola T, Forrester N, Gould EA, Lafitte D, Ferron F, Lescar J, Gorbalenya AE, de Lamballerie X, Canard B. 2009. The crystal structures of chikungunya and Venezuelan equine encephalitis virus nsP3 macro domains define a conserved adenosine binding pocket. J Virol 83:6534–6545. https://doi.org/10.1128/JVI.00189-09.
19. Shin G, Yost SA, Miller MT, Elrod EJ, Grakoui A, Marcotrigiano J. 2012. Structural and functional insights into alphavirus polyprotein processing and pathogenesis. Proc Natl Acad Sci U S A 109:16534–16539. https://doi.org/10.1073/pnas.1210418109.
20. Eckei L, Krieg S, Butepage M, Lehmann A, Gross A, Lippok B, Grimm AR, Kummerer BM, Rossetti G, Luscher B, Verheugd P. 2017. The conserved macrodomains of the non-structural proteins of chikungunya virus and other pathogenic positive strand RNA viruses function as mono-ADP-ribosylhydrolases. Sci Rep 7:41746. https://doi.org/10.1038/srep41746.
21. McPherson RL, Abraham R, Sreekumar E, Ong SE, Cheng SJ, Baxter VK, Kistemaker HA, Filippov DV, Griffin DE, Leung AK. 2017. ADP-ribosylhydrolase activity of chikungunya virus macrodomain is critical for virus replication and virulence. Proc Natl Acad Sci U S A 114:1666–1671. https://doi.org/10.1073/pnas.1621485114.
22. Leung AKL, McPherson RL, Griffin DE. 2018. Macrodomain ADP-ribosylhydrolase and the pathogenesis of infectious diseases. PLoS Pathog 14:e1006864. https://doi.org/10.1371/journal.ppat.1006864.
23. Akhrymuk I, Frolov I, Frolova EI. 2018. Sindbis virus infection causes cell death by nsP2-induced transcriptional shutoff or by nsP3-dependent translational shutoff. J Virol 92:e01388-18. https://doi.org/10.1128/JVI.01388-18.
24. Akhrymuk I, Lukash T, Frolov I, Frolova EI. 2019. Novel mutations in nsP2 abolish chikungunya virus-induced transcriptional shutoff and make the virus less cytopathic without affecting its replication rates. J Virol 93:e02062-18. https://doi.org/10.1128/JVI.02062-18.
25. Meshram CD, Lukash T, Phillips AT, Akhrymuk I, Frolova EI, Frolov I. 2019. Lack of nsP2-specific nuclear functions attenuates chikungunya virus replication both in vitro and in vivo. Virology 534:14–24. https://doi.org/10.1016/j.virol.2019.05.016.
26. LaStarza MW, Lemm JA, Rice CM. 1994. Genetic analysis of the nsP3 region of Sindbis virus: evidence for roles in minus-strand and subgenomic RNA synthesis. J Virol 68:5781–5791.
27. Foy NJ, Akhrymuk M, Shustov AV, Frolova EI, Frolov I. 2013. Hypervariable domain of nonstructural protein nsP3 of Venezuelan equine encephalitis virus determines cell-specific mode of virus replication. J Virol 87:7569–7584. https://doi.org/10.1128/JVI.00720-13.
28. De I, Fata-Hartley C, Sawicki SG, Sawicki DL. 2003. Functional analysis of nsP3 phosphoprotein mutants of Sindbis virus. J Virol 77:13106–13116. https://doi.org/10.1128/jvi.77.24.13106-13116.2003.
29. Vihinen H, Saarinen J. 2000. Phosphorylation site analysis of Semliki Forest virus nonstructural protein 3. J Biol Chem 275:27775–27783. https://doi.org/10.1074/jbc.M002195200.
30. Frolova E, Gorchakov R, Garmashova N, Atasheva S, Vergara LA, Frolov I. 2006. Formation of nsP3-specific protein complexes during Sindbis virus replication. J Virol 80:4122–4134. https://doi.org/10.1128/JVI.80.8.4122-4134.2006.
31. Kim DY, Reynaud JM, Rasalouskaya A, Akhrymuk I, Mobley JA, Frolov I, Frolova EI. 2016. New World and Old World alphaviruses have evolved to exploit different components of stress granules, FXR and G3BP proteins, for assembly of viral replication complexes. PLoS Pathog 12:e1005810. https://doi.org/10.1371/journal.ppat.1005810.
32. Scholte FE, Tas A, Albulescu IC, Zusinaite E, Merits A, Snijder EJ, van Hemert MJ. 2015. Stress granule components G3BP1 and G3BP2 play a proviral role early in chikungunya virus replication. J Virol 89:4457–4469. https://doi.org/10.1128/JVI.03612-14.
33. Frolov I, Kim DY, Akhrymuk M, Mobley JA, Frolova EI. 2017. Hypervariable domain of Eastern equine encephalitis virus nsP3 redundantly utilizes multiple cellular proteins for replication complex assembly. J Virol 91:e00371-17. https://doi.org/10.1128/JVI.00371-17.
34. Meshram CD, Agback P, Shiliaev N, Urakova N, Mobley JA, Agback T, Frolova EI, Frolov I. 2018. Multiple host factors interact with the hypervariable domain of chikungunya virus nsP3 and determine viral replication in cell-specific mode. J Virol 92:e00838-18. https://doi.org/10.1128/JVI.00838-18.
35. Mutso M, Morro AM, Smedberg C, Kasvandik S, Aquilimeba M, Teppor M, Tarve L, Lulla A, Lulla V, Saul S, Thaa B, McInerney GM, Merits A, Varjak M. 2018. Mutation of CD2AP and SH3KBP1 binding motif in alphavirus nsP3 hypervariable domain results in attenuated virus. Viruses 10:E226. https://doi.org/10.3390/v10050226.
36. Fros JJ, Domeradzka NE, Baggen J, Geertsema C, Flipse J, Vlak JM, Pijlman GP. 2012. Chikungunya virus nsP3 blocks stress granule assembly by recruitment of G3BP into cytoplasmic foci. J Virol 86:10873–10879. https://doi.org/10.1128/JVI.01506-12.
37. Frolova EI, Gorchakov R, Pereboeva L, Atasheva S, Frolov I. 2010. Functional Sindbis virus replicative complexes are formed at the plasma membrane. J Virol 84:11679–11695. https://doi.org/10.1128/JVI.01441-10.
38. Schulte T, Liu L, Panas MD, Thaa B, Dickson N, Gotte B, Achour A, McInerney GM. 2016. Combined structural, biochemical and cellular evidence demonstrates that both FGDF motifs in alphavirus nsP3 are required for efficient replication. Open Biol 6:160078. https://doi.org/10.1098/rsob.160078.
39. Panas MD, Ahola T, McInerney GM. 2014. The C-terminal repeat domains of nsP3 from the Old World alphaviruses bind directly to G3BP. J Virol 88:5888–5893. https://doi.org/10.1128/JVI.00439-14.
40. Agback P, Dominguez F, Pustovalova Y, Lukash T, Shiliaev N, Orekhov VY, Frolov I, Agback T, Frolova EI. 2019. Structural characterization and biological function of bivalent binding of CD2AP to intrinsically disordered domain of chikungunya virus nsP3 protein. Virology 537:130–142. https://doi.org/10.1016/j.virol.2019.08.022.
41. Foy NJ, Akhrymuk M, Akhrymuk I, Atasheva S, Bopda-Waffo A, Frolov I, Frolova EI. 2013. Hypervariable domains of nsP3 proteins of New World and Old World alphaviruses mediate formation of distinct, virus-specific protein complexes. J Virol 87:1997–2010. https://doi.org/10.1128/JVI.02853-12.
42. Urakova N, Kuznetsova V, Crossman DK, Sokratian A, Guthrie DB, Kolykhalov AA, Lockwood MA, Natchus MG, Crowley MR, Painter GR, Frolova EI, Frolov I. 2018. β-D-N^4-Hydroxycytidine is a potent anti-alphavirus compound that induces a high level of mutations in the viral genome. J Virol 92:e01965-17. https://doi.org/10.1128/JVI.01965-17.
43. Hyde JL, Gardner CL, Kimura T, White JP, Liu G, Trobaugh DW, Huang C, Tonelli M, Paessler S, Takeda K, Klimstra WB, Amarasinghe GK, Diamond MS. 2014. A viral RNA structural element alters host recognition of nonself RNA. Science 343:783–787. https://doi.org/10.1126/science.1248465.
44. Reynaud JM, Kim DY, Atasheva S, Rasalouskaya A, White JP, Diamond MS, Weaver SC, Frolova EI, Frolov I. 2015. IFIT1 differentially interferes with translation and replication of alphavirus genomes and promotes induction of type I interferon. PLoS Pathog 11:e1004863. https://doi.org/10.1371/journal.ppat.1004863.

45. Davis NL, Powell N, Greenwald GF, Willis LV, Johnson BJB, Smith JF, Johnston RE. 1991. Attenuating mutations in the E2 glycoprotein gene of Venezuelan equine encephalitis: construction of single and multiple mutants in a full-length clone. Virology 183:20–31. https://doi.org/10.1016/0042-6822(91)90114-Q.
46. Kulasegaran-Shylini R, Thiviyanathan V, Gorenstein DG, Frolov I. 2009. The 5′UTR-specific mutation in VEEV TC-83 genome has a strong effect on RNA replication and subgenomic RNA synthesis, but not on translation of the encoded proteins. Virology 387:211–221. https://doi.org/10.1016/j.virol.2009.02.027.
47. Gorchakov R, Garmashova N, Frolova E, Frolov I. 2008. Different types of nsP3-containing protein complexes in Sindbis virus-infected cells. J Virol 82:10088–10101. https://doi.org/10.1128/JVI.01011-08.
48. Tossavainen H, Aitio O, Hellman M, Saksela K, Permi P. 2016. Structural basis of the high affinity interaction between the alphavirus nonstructural protein-3 (nsP3) and the SH3 domain of amphiphysin-2. J Biol Chem 291:16307–16317. https://doi.org/10.1074/jbc.M116.732412.
49. Gotte B, Liu L, McInerney GM. 2018. The enigmatic alphavirus nonstructural protein 3 (nsP3) revealing its secrets at last. Viruses 10:E105. https://doi.org/10.3390/v10030105.
50. Nasar F, Palacios G, Gorchakov RV, Guzman H, Da Rosa AP, Savji N, Popov VL, Sherman MB, Lipkin WI, Tesh RB, Weaver SC. 2012. Eilat virus, a unique alphavirus with host range restricted to insects by RNA replication. Proc Natl Acad Sci U S A 109:14622–14627. https://doi.org/10.1073/pnas.1204787109.
51. Nasar F, Gorchakov RV, Tesh RB, Weaver SC. 2015. Eilat virus host range restriction is present at multiple levels of the virus life cycle. J Virol 89:1404–1418. https://doi.org/10.1128/JVI.01856-14.
52. Alevizatos AC, McKinney RW, Feigin RD. 1967. Live, attenuated Venezuelan equine encephalomyelitis virus vaccine. I. Clinical effects in man. Am J Trop Med Hyg 16:762–768. https://doi.org/10.4269/ajtmh.1967.16.762.
53. Berge TO, Banks IS, Tigertt WD. 1961. Attenuation of Venezuelan equine encephalomyelitis virus by in vitro cultivation in guinea pig heart cells. Am J Hyg 73:209–218. https://doi.org/10.1093/oxfordjournals.aje.a120178.
54. Atasheva S, Kim DY, Akhrymuk M, Morgan DG, Frolova EI, Frolov I. 2013. Pseudoinfectious Venezuelan equine encephalitis virus: a new means of alphavirus attenuation. J Virol 87:2023–2035. https://doi.org/10.1128/JVI.02881-12.
55. Atasheva S, Kim DY, Frolova EI, Frolov I. 2015. Venezuelan equine encephalitis virus variants lacking transcription inhibitory functions demonstrate highly attenuated phenotype. J Virol 89:71–82. https://doi.org/10.1128/JVI.02252-14.
56. Garmashova N, Atasheva S, Kang W, Weaver SC, Frolova E, Frolov I. 2007. Analysis of Venezuelan equine encephalitis virus capsid protein function in the inhibition of cellular transcription. J Virol 81:13552–13565. https://doi.org/10.1128/JVI.01576-07.
57. Kim DY, Firth AE, Atasheva S, Frolova EI, Frolov I. 2011. Conservation of a packaging signal and the viral genome RNA packaging mechanism in alphavirus evolution. J Virol 85:8022–8036. https://doi.org/10.1128/JVI.00644-11.
58. Atasheva S, Krendelchtchikova V, Liopo A, Frolova E, Frolov I. 2010. Interplay of acute and persistent infections caused by Venezuelan equine encephalitis virus encoding mutated capsid protein. J Virol 84:10004–10015. https://doi.org/10.1128/JVI.01151-10.
59. Atasheva S, Garmashova N, Frolov I, Frolova E. 2008. Venezuelan equine encephalitis virus capsid protein inhibits nuclear import in mammalian but not in mosquito cells. J Virol 82:4028–4041. https://doi.org/10.1128/JVI.02330-07.
60. Kim DY, Atasheva S, Foy NJ, Wang E, Frolova EI, Weaver S, Frolov I. 2011. Design of chimeric alphaviruses with a programmed, attenuated, cell type-restricted phenotype. J Virol 85:4363–4376. https://doi.org/10.1128/JVI.00065-11.
61. Kim DY, Atasheva S, Frolova EI, Frolov I. 2013. Venezuelan equine encephalitis virus nsP2 protein regulates packaging of the viral genome into infectious virions. J Virol 87:4202–4213. https://doi.org/10.1128/JVI.03142-12.
62. Anishchenko M, Paessler S, Greene IP, Aguilar PV, Carrara AS, Weaver SC. 2004. Generation and characterization of closely related epizootic and enzootic infectious cDNA clones for studying interferon sensitivity and emergence mechanisms of Venezuelan equine encephalitis virus. J Virol 78:1–8. https://doi.org/10.1128/jvi.78.1.1-8.2004.
63. Gorchakov R, Frolova E, Williams BR, Rice CM, Frolov I. 2004. PKR-dependent and -independent mechanisms are involved in translational shutoff during Sindbis virus infection. J Virol 78:8455–8467. https://doi.org/10.1128/JVI.78.16.8455-8467.2004.
64. Bredenbeek PJ, Frolov I, Rice CM, Schlesinger S. 1993. Sindbis virus expression vectors: packaging of RNA replicons by using defective helper RNAs. J Virol 67:6439–6446.
65. Liljeström P, Lusa S, Huylebroeck D, Garoff H. 1991. *In vitro* mutagenesis of a full-length cDNA clone of Semliki Forest virus: the small 6,000-molecular-weight membrane protein modulates virus release. J Virol 65:4107–4113.
66. Gorchakov R, Hardy R, Rice CM, Frolov I. 2004. Selection of functional 5′ cis-acting elements promoting efficient Sindbis virus genome replication. J Virol 78:61–75. https://doi.org/10.1128/jvi.78.1.61-75.2004.
67. Lemm JA, Durbin RK, Stollar V, Rice CM. 1990. Mutations which alter the level or structure of nsP4 can affect the efficiency of Sindbis virus replication in a host-dependent manner. J Virol 64:3001–3011.